

Ammonium Sulfate and Ultrafine Particle Affect early Onset of Alzheimer's Disease

Samal Kaumbekova*, Mehdi Amouei Torkmahalleh, Dhawal Shah

Department of Chemical and Materials Engineering, School of Engineering and Digital Sciences, Nazarbayev University, Nur – Sultan, Kazakhstan.
 skaumbekova@nu.edu.kz

Recent environmental studies have shown the impact of air quality on human health and in particular, toxicological effect of particulate matter (PM) and ultrafine particles (UFPs) on progression of neurodegenerative diseases. While in-vivo experiments reveal enhanced concentration of amyloid beta peptides in the brains of animals after the exposure to PM and UFPs, the molecular interactions between peptides and atmospheric pollutants remain obscure. In this study, molecular dynamics simulations were performed to investigate the effect of UFPs on the aggregation of amyloid beta peptides, associated with the development of Alzheimer's Disease (AD) in human brain. In particular, the changes in the structure of eight A β_{16-21} peptides, the segment of A β_{1-42} peptide with the high propensity to aggregate were investigated. The aggregation kinetics of A β_{16-21} peptides and amount of beta sheets in their secondary structures were studied in the presence of varying concentrations of NH $_4^+$ and SO $_4^{2-}$ ions, common secondary inorganic ions found in the environmental realm from the different sources of atmospheric pollution. Moreover, the effect of hydrophobic UFP, modelled by C $_{60}$ molecule, on the structure of peptides was analysed. The aggregation kinetics was calculated by estimating the time necessary to reach Solvent Accessible Surface Area (SASA) of peptides of 60 nm 2 . The study demonstrated that, although, the inhibitory effect of hydrophobic UFP on the formation of beta sheets was revealed, there could be a synergistic effect of the concentration of (NH $_4$) $_2$ SO $_4$ salt and presence of UFP on the aggregation kinetics of peptides. Among three different salt concentrations of 0.15 M, 0.25 M and 0.35 M, the slowest aggregation of peptides in the absence of C $_{60}$ molecule and the fastest aggregation in the presence of C $_{60}$ were observed at 0.25 M of (NH $_4$) $_2$ SO $_4$.

1. Introduction

The impact of indoor and outdoor air quality on human health is one of the significant issues under the interest of the environmental odour control nowadays. The main constituents of the urban air pollution are volatile organic compounds, organic and elemental carbon, polycyclic aromatic hydrocarbons, ammonium, nitrates, sulfates, chlorides, crustal and trace elements (Chen, et al. 2016). The concentrations and the size of the particles in the atmosphere, as well as the composition of the pollutants is complex, depending on the source of the pollution in a particular region. For instance, a sampling showed that the major constituents of the ultrafine particulate matter in California were organic and elemental carbon, while sulfur had the highest abundancy among other trace elements measured in this region (Xue, et al. 2020). In addition, the studies showed that burning of natural gas and methane produces high amounts of the particles with the dimensions of 2 – 3 nm (Minutolo, et al. 2010). The recent studies have showed that environmental pollutants and particulate matter (PM) have negative effect on human organism and may contribute to the development of asthma, lung cancer, diabetes and other illnesses of the respiratory, cardiovascular and cardiopulmonary systems (Losacco and Perillo 2018). Moreover, particles of the lower size, such as ultrafine particles (UFPs), with the size of lower than 100 nm, may pass the blood – brain barrier upon being inhaled and result in progression of neurodegenerative diseases (Oberdörster, et al. 2004).

Alzheimer's Disease is a neurodegenerative disease, associated with the loss of cognitive and motor skills in elder people. The disease is related to the formation of amyloid plaques in the human brain from the aggregation of amyloid beta (A β) peptides to amyloid fibrils with the enhanced amount of beta sheets

(Cheignon, et al. 2018). Amyloid beta peptides are produced from APP (amyloid precursor protein) and have 38 - 43 aminoacids in their structure (Andreeva, Lukiw, and Rogaev 2017).

The in-vivo studies illustrated that exposure to PM_{2.5} for 9 months increased the concentration of A β ₁₋₄₀ peptides in the brain of mouse (Bhatt, et al. 2015). Moreover, the recent study showed the enhanced amount of A β peptides observed in the hippocampus of mice due to the exposure to UFPs for 3 weeks (Park, et al. 2020). One of the limitations of the experimental studies is that the molecular interactions between the atmospheric pollutants and A β peptides remain obscure. Moreover, due to the complex composition of PM and UFPs, it is also under high interest to identify the pollutants that have the highest contribution to the early development and progression of Alzheimer's Disease (Kilian and Kitazawa 2018). In this respect, a systematic study is required to investigate the effect of environmental pollutants and their concentrations on the aggregation of amyloid beta peptides in human brain.

Molecular Dynamics (MD) simulations is a computational approach aimed to study the interactions between particles on the molecular level, that allows to look at the interactions between amyloid beta peptides and environmental pollutants. Recent MD study on the structure of A β ₄₂ peptide in the presence of environmental toxic gases showed that the structure of the peptide was stabilized in the presence of SO₂, CO, CO₂ and NO₂ gases, hypothesizing that the aggregation of amyloid beta peptides would be increased in the presence of the environmental pollutants (Saranya, et al. 2020).

In the present MD study, the aggregation of eight A β ₁₆₋₂₁ peptides, the segment of the amyloid beta peptide with the high aggregation propensity (Sun, et al. 2017), was chosen to investigate the aggregation of A β peptides in the absence and presence of hydrophobic UFP, mimicked by C₆₀ molecule. The MD simulations were performed in the presence of different concentrations of NH₄⁺ and SO₄⁻² ions, typical environmental pollutants found in the environmental realm from the agricultural activities and combustion sources. It was hypothesised that the composition and various concentrations of environmental pollutants would have effect on the amounts of beta sheets and hydrogen bonds observed in the secondary structure of A β peptides and the kinetics of their aggregation.

2. Methodology

GROMACS v2018.3 was used to perform all atom molecular dynamics simulations with the gromos54a7 forcefield parameters, used for the simulations of A β peptides with validated results in-vitro (Gerben, et al. 2014). The coordinates of A β ₁₆₋₂₁ peptide with the aminoacid sequence of KLVFFA were taken from the Protein Data Bank with the PDB ID: 2Y2A (Colletier, et al. 2011). For all systems under the study, a simulation box with the dimensions of 7 \times 7 \times 7 nm³ was created and filled by the desired number of molecules, as shown in Table 1.

Table 1: Systems under the study with the number of molecules and specified salt concentrations in the simulation box, with three runs repeated for each system.

System	A β ₁₆₋₂₁ peptide	C ₆₀	(NH ₄) ₂ SO ₄ salt concentration	H ₂ O
1	8	-	0.15 M	10,828 \pm 13
2	8	1	0.15 M	10,819 \pm 17
3	8	-	0.25 M	10,743 \pm 7
4	8	1	0.25 M	10,729 \pm 5
5	8	-	0.35 M	10,680 \pm 16
6	8	1	0.35 M	10,669 \pm 5

As shown in Table 1, eight A β ₁₆₋₂₁ peptides were inserted in the simulation box to investigate the aggregation of the peptides at six different conditions, keeping the concentration of the peptides at 38.8 mM. The spc/e model of water molecules was used to fully solvate the simulation box. One C₆₀ molecule was added to mimic a hydrophobic ultrafine particle in systems 2, 4 and 6, that corresponds to 4.843 mM concentration of C₆₀ in the simulation box. In addition, to investigate the effect of (NH₄)₂SO₄ salt concentration on the aggregation of amyloid beta peptides, the salt concentrations were varied from 0.15 M (systems 1 and 2) to 0.25 M (systems 3 and 4) and 0.35 M (systems 5 and 6), by changing the number of ions in the simulation box. It should be noted, that due to the limitations of the molecular modeling, the concentrations of UFP and ions used in this study were different from those found in human blood. However, it should be expected that long-time exposure to environmental pollutants of high concentrations would result in higher amounts of particles in the blood serum of human organism. Moreover, the obtained results are promising in terms of elucidation of the secondary structures of peptides and their aggregation pathways at different compositions of air pollutants in the simulation box.

After all molecules were randomly inserted in the simulation box, energy minimization step was performed to optimize the starting parameters, setting maximum force on any atom to 500 kJ/mol/nm and applying periodic boundary conditions in three axes. Furthermore, the equilibration was performed by NVT - equilibration step for 0.1 ns at constant temperature of 298 K, followed by NPT – equilibration step for 0.1 ns, setting constant pressure at 1 bar and constant temperature at 298 K. Afterwards, the molecular dynamics run was performed for 50 ns with the integration time step of 0.002 ps. For the simulations, LINCS algorithm was used for all bond constraints and the cut-off distance of 1.0 nm was indicated for Lennard – Jones potential and Coulomb interactions. All six systems under the study were simulated three times starting from the step of randomly inserting the specified number of molecules.

After the production run, VMD (Visual Molecular Dynamics) software was used to visualize the systems under the study. To characterize the interactions between the peptides, the number of hydrogen bonds for the last 10 ns of the md simulation was quantified taking the average between three runs for all systems. In addition, the secondary structure of the A β ₁₆₋₂₁ peptides was studied by indicating the average percentage amount of the beta sheets observed in their structure in the last 10 ns of the simulation. Furthermore, the aggregation of eight A β ₁₆₋₂₁ peptides was studied by analyzing Solvent Accessible Surface Area (SASA) of the peptides. Particularly, the regression lines of the plots generated from SASA analysis from all runs were fitted by the polynomial fit with up to 5th order. To compare the aggregation kinetics of the peptides among six systems under the study, the produced regression line equations with the polynomial fit were further used to estimate the time when the SASA of the peptides would reach the values of 60 nm² and 55 nm² in all systems, taking the average of two runs with the highest values of R² for each system.

3. Results and Discussion

The visualization of the systems under the study by VMD software showed the aggregation of eight A β ₁₆₋₂₁ peptides was accomplished within 50 ns of the md simulation run. Moreover, it was noted that during the simulation, C₆₀ molecule was also bound to the peptides due to the hydrophobic interactions, resulted in the formation of a larger aggregate of the peptides and UFP. The representative snapshots of systems 1 and 2 with 0.15 M (NH₄)₂SO₄ salt in the simulation box before and after the md run are shown on Figure 1.

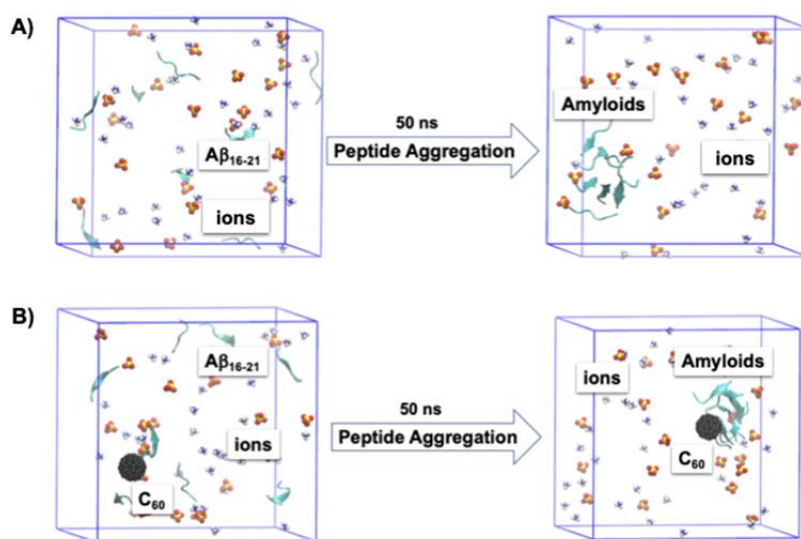


Figure 1: Representative snapshot of A) system 1 and B) system 2, before and after 50 ns (cyan: eight A β ₁₆₋₂₁ peptides, black: C₆₀, blue and white: NH₄⁺ ions, red and yellow: SO₄⁻² ions; water molecules are not shown).

To investigate the interactions between eight A β ₁₆₋₂₁ peptides in six different systems under the study, the change in the average number of hydrogen bonds observed between the peptides was studied for 50 ns of the simulations, illustrated on Figure 2.

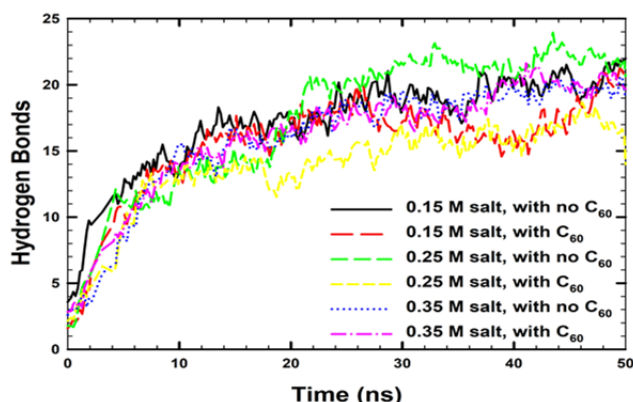


Figure 2: Average number of hydrogen bonds observed between eight $A\beta_{16-21}$ peptides in six different systems under the study.

According to results of H – bonds analysis, as shown on Figure 2, the average number of hydrogen bonds between peptides in the systems under the study was increased from the value of 2.6 ± 0.8 in the beginning of the simulation to the value of 19.4 ± 2.8 after 50 ns of the md run. The results indicated that the interactions between the peptides were increased during the simulation, in agreement with the observed aggregation of the peptides from the visualization of the systems. Moreover, the average number of H – bonds and average percentage amounts of the beta sheets in the structure of the peptides were studied for the last 10 ns of the simulation, when the systems were stabilized, shown in Table 2.

Table 2: Average number of hydrogen bonds and average percentage number of beta sheets observed between 8 amyloid β_{16-21} peptides in $(NH_4)_2SO_4$ salt in the last 10 ns of the simulations.

System	C_{60}	$(NH_4)_2SO_4$ Salt concentration	H - bonds	Beta sheets
1	-	0.15 M	20.4 ± 1.3	28 %
2	1	0.15 M	18.0 ± 2.1	20 %
3	-	0.25 M	22.0 ± 1.3	21 %
4	1	0.25 M	16.9 ± 1.3	14 %
5	-	0.35 M	19.6 ± 1.2	24 %
6	1	0.35 M	20.3 ± 1.2	20 %

According to Table 2, for the last 10 ns of the simulation, at 0.15 M and 0.25 M salt concentrations, the average number of H – bonds between amyloid beta peptides were reduced in the presence of C_{60} , system 2 (18.0 ± 2.1) and system 4 (16.9 ± 1.3), in comparison to the corresponding systems with the similar salt concentrations and no UFP, system 1 (20.4 ± 1.3) and system 3 (22.0 ± 1.3), respectively. In contrast, at 0.35 M salt concentration, the higher amount of H – bonds between peptides were observed in the presence of C_{60} , in system 6 (20.3 ± 1.2), in comparison to system 5 (19.6 ± 1.2) with no UFP. It was also noted, that among all six systems under the study, the highest amount of H – bonds were observed in system 3, while the lowest interactions were noticed in system 4.

According to the analysis of the beta sheets observed in the peptides in the last 10 ns of the simulation, at all concentrations of $(NH_4)_2SO_4$ salt, the average percentage amount of beta sheets was reduced in the presence of C_{60} due to the hydrophobic interactions of the peptides with UFP. Presence of UFP in the simulation box resulted in the formation of less ordered structures of the peptides in systems 2 and 6 (20% of beta sheets), and system 4 (14%), in comparison to the corresponding systems with the same salt concentration and no UFP, systems 1, 3 and 5 with 28%, 21% and 24% of beta sheets in the structure of the peptides, respectively. A possible explanation could be that binding of the peptides to UFP resulted in the formation of less ordered structures of the peptides on the surface of C_{60} , as shown on Figure 1. In addition, among all salt concentrations, the lowest amount of the beta sheets was observed at 0.25 M salt concentration, in system 3 (21%) and system 4 (14%).

Next, to characterize the aggregation kinetics of the peptides, the changes in the SASA of eight $A\beta_{16-21}$ peptides during 50 ns of the simulation were analyzed. In the beginning of the md run, the SASA values were approximately 83 nm^2 , which was decreased to $\sim 43 \text{ nm}^2$ after 50 ns of the simulation. The significant decrease in the surface area of the peptides available for the solvent also confirmed that the aggregation of peptides occurred during the simulation. The deviations in the SASA values of the peptides observed during three molecular dynamics runs of system 1 are shown on Figure 3.

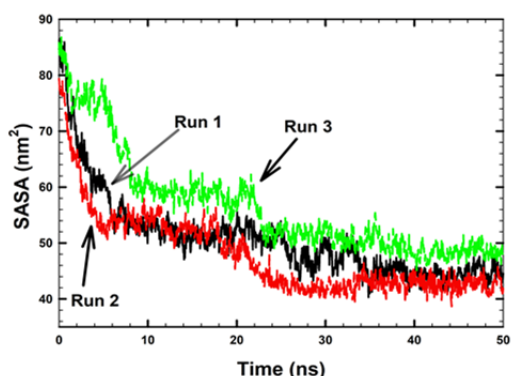


Figure 3: Total SASA of eight $A\beta_{16-21}$ peptides in the presence of 0.15 M $(NH_4)_2SO_4$ salt for the three runs of system 1.

According to Figure 3, for all three runs the deviations in the SASA values were significantly higher in the beginning of the simulation with the smaller fluctuations observed towards the end of the run, indicating that the system was stabilized during the last 10 ns of the simulation with the completion of the aggregation of the peptides. The aggregation kinetics was further studied by fitting the trendline of SASA plot with a polynomial fit for all three runs of all systems. The trendline equations that characterized the deviations in the SASA of the peptides from three different runs of system 1 are shown in Table 3.

Table 3: Characterization of the total SASA of eight $A\beta_{16-21}$ peptides in the presence of 0.15 M $(NH_4)_2SO_4$ salt for three runs of system 1.

Run	SASA at 0 ns	SASA at 50 ns	Regression Line Equation	R^2
1	84.644 nm ²	44.554 nm ²	$-3 \times 10^{-21} X^5 + 5 \times 10^{-16} X^4 - 3 \times 10^{-11} X^3 + 7 \times 10^{-7} X^2 - 0.0075 X + 83.129$	0.9464
2	79.365 nm ²	42.122 nm ²	$-5 \times 10^{-21} X^5 + 6 \times 10^{-16} X^4 - 3 \times 10^{-11} X^3 + 6 \times 10^{-7} X^2 - 0.0056 X + 73.597$	0.903
3	85.787 nm ²	47.813 nm ²	$-8 \times 10^{-22} X^5 + 1 \times 10^{-16} X^4 - 8 \times 10^{-12} X^3 + 2 \times 10^{-7} X^2 - 0.004 X + 85.304$	0.9395

From the obtained regression line equations for three runs of system 1 (Table 3), the time necessary to reach SASA of 60 and 55 nm² was estimated by taking the average among two runs with the highest R^2 parameter. To compare the aggregation kinetics of the peptides in six different environments, a similar procedure was used. The results of the estimated aggregation kinetics of the peptides in six different systems under the study are shown in Table 4.

Table 4: Average time to reach a total SASA of 60 nm² and 55 nm² by 8 amyloid β_{16-21} peptides in the systems with $(NH_4)_2SO_4$ salt taken from the two systems with highest R^2 .

System	C ₆₀	$(NH_4)_2SO_4$ Salt concentration	Time at SASA of 60 nm ²	Time at SASA of 55 nm ²
1	-	0.15 M	7.0 ± 3.0 ns	9.6 ± 2.8 ns
2	1	0.15 M	13.8 ± 3.2 ns	18.0 ± 4.2 ns
3	-	0.25 M	13.0 ± 1.6 ns	16.8 ± 3.0 ns
4	1	0.25 M	9.0 ± 1.8 ns	11.2 ± 1.4 ns
5	-	0.35 M	7.7 ± 0.7 ns	9.8 ± 1.3 ns
6	1	0.35 M	9.5 ± 1.7 ns	12.4 ± 0.9 ns

According to Table 4, in the absence of C60, the slowest aggregation of eight $A\beta_{16-21}$ peptides was observed in system 3 with 0.25 M salt concentration among three different concentrations. While in the presence of UFP, the slowest aggregation of the peptides occurred in system 1 with 0.15 M salt concentration in comparison to systems 3 and 5 with different salt concentrations. Furthermore, it was noted that at 0.15 M and 0.35 M salt concentrations, the aggregation kinetics of the peptides was approximately 50% slower in the presence of C60 molecule in system 2 (SASA₆₀ = 13.8 ± 3.2 ns) and for approximately 20% in system 6 (SASA₆₀ = 9.5 ± 1.7 ns), in comparison to the corresponding systems with the similar salt concentrations with no UFP, system 1 (SASA₆₀ = 7.0 ± 3.0 ns) and system 5 (SASA₆₀ = 7.7 ± 0.7 ns). The reason could be binding of C60 to peptides, as shown on Figure 1, that obstructed the peptides from binding to each other. In complete contrast, at 0.25 M salt concentration, the aggregation became faster for approximately 30% in the presence of C60, in system 4 (SASA₆₀ = 9.0 ± 1.8 ns), in comparison to the corresponding system with no

UFP, system 3 (SASA60 = 13.0 ± 1.6 ns). This observation illustrated presence of a synergistic effect of salt concentration and presence of UFP on the aggregation kinetics of the peptides.

4. Conclusions

To conclude, in the present MD study, eight A β ₁₆₋₂₁ peptides produced an amyloid aggregate, that was confirmed by the visualization, increase in the number of H – bonds and decrease in SASA of peptides within 50 ns of the simulation time. Moreover, hydrophobic UFP, modelled by C₆₀ molecule also was bound to peptides, resulted in the reduced amounts of beta sheets observed in the peptides after the simulations at all ammonium sulfate salt concentrations. The number of H – bonds between the peptides were also decreased in the presence of UFP at 0.15 M and 0.25 M ammonium sulfate salt concentrations, however, increased at 0.35 M (NH₄)₂SO₄. The most significant decrease (50%) in the aggregation kinetics due to the presence of UFP, was observed at 0.15 M of (NH₄)₂SO₄. In contrast, the aggregation of peptides was faster for 30% in the presence of C₆₀ at 0.25 M salt concentration. Nevertheless, no correlation between the aggregation kinetics of the peptides and the amount of hydrogen bonds and beta sheets in the secondary structure of peptides was noticed in this study.

References

- Andreeva, T. V., W. J. Lukiw, and E. I. RogaeV. 2017. "Biological Basis for Amyloidogenesis in Alzheimer's Disease." *Biochemistry (Mosc)* 82, no. 2 (Feb): 122-139. <http://dx.doi.org/10.1134/S0006297917020043>.
- Bhatt, D. P., et al. 2015. "A Pilot Study to Assess Effects of Long-Term Inhalation of Airborne Particulate Matter on Early Alzheimer-Like Changes in the Mouse Brain." *PLoS One* 10, no. 5: e0127102. <http://dx.doi.org/10.1371/journal.pone.0127102>.
- Cheignon, C., et al. 2018. "Oxidative Stress and the Amyloid Beta Peptide in Alzheimer's Disease." *Redox Biology* 14 (2018/04/01): 450-464. <http://dx.doi.org/https://doi.org/10.1016/j.redox.2017.10.014>.
- Chen, R., et al. 2016. "Beyond Pm2.5: The Role of Ultrafine Particles on Adverse Health Effects of Air Pollution." *Biochim Biophys Acta* 1860, no. 12 (12): 2844-55. <http://dx.doi.org/10.1016/j.bbagen.2016.03.019>.
- Colletier, Jacques-Philippe, et al. 2011. "Molecular Basis for Amyloid-B Polymorphism." *Proceedings of the National Academy of Sciences* 108, no. 41: 16938. <http://dx.doi.org/10.1073/pnas.1112600108>.
- Gerben, S. R., et al. 2014. "Comparing Atomistic Molecular Mechanics Force Fields for a Difficult Target: A Case Study on the Alzheimer's Amyloid B-Peptide." *Journal of Biomolecular Structure and Dynamics* 32, no. 11: 1817-32. <http://dx.doi.org/10.1080/07391102.2013.838518>.
- Kilian, J., and M. Kitazawa. 2018. "The Emerging Risk of Exposure to Air Pollution On cognitive Decline and Alzheimer's Disease - Evidence from Epidemiological and Animal Studies." *Biomed J* 41, no. 3 (06): 141-162. <http://dx.doi.org/10.1016/j.bj.2018.06.001>.
- Losacco, C., and A. Perillo. 2018. "Particulate Matter Air Pollution and Respiratory Impact on Humans and Animals." *Environ Sci Pollut Res Int* 25, no. 34 (Dec): 33901-33910. <http://dx.doi.org/10.1007/s11356-018-3344-9>.
- Minutolo, P., et al. 2010. "Ultrafine Particle Emission from Combustion Devices Burning Natural Gas." *Chemical Engineering Transactions* 22: 239-244. <https://doi.org/10.3303/CET1022039>
- Oberdörster, G., et al. 2004. "Translocation of Inhaled Ultrafine Particles to the Brain." *Inhal Toxicol* 16, no. 6-7 (Jun): 437-45. <http://dx.doi.org/10.1080/08958370490439597>.
- Park, S. J., et al. 2020. "Exposure of Ultrafine Particulate Matter Causes Glutathione Redox Imbalance in the Hippocampus: A Neurometabolic Susceptibility to Alzheimer's Pathology." *Science of the Total Environment* 718 (May): 137267. <http://dx.doi.org/10.1016/j.scitotenv.2020.137267>.
- Saranya, V., et al. 2020. "The Hazardous Effects of the Environmental Toxic Gases on Amyloid Beta-Peptide Aggregation: A Theoretical Perspective." *Biophysical Chemistry* 263 (Aug): 106394. <http://dx.doi.org/10.1016/j.bpc.2020.106394>.
- Sun, Y., et al. 2017. "Distinct Oligomerization and Fibrillization Dynamics of Amyloid Core Sequences of Amyloid-Beta and Islet Amyloid Polypeptide." *Physical Chemistry Chemical Physics* 19, no. 41 (Oct): 28414-28423. <http://dx.doi.org/10.1039/c7cp05695h>.
- Xue, Wei, et al. 2020. "Day-of-Week Patterns for Ultrafine Particulate Matter Components at Four Sites in California." *Atmospheric Environment* 222 (2020/02/01): 117088. <http://dx.doi.org/https://doi.org/10.1016/j.atmosenv.2019.117088>.